Eleventh International Conference on CFD in the Minerals and Process Industries
CSIRO, Melbourne, Australia
7-9 December 2015

MULTIPHASE TRANSPORT IN THE SMALL INTESTINE

Matthew D. SINNOTT[1,2*], Paul W. CLEARY[1,2] and Simon M. HARRISON[1,2]

[1]CSIRO Data61, Clayton, Victoria 3169, AUSTRALIA
[2]CSIRO Food and Nutrition, Clayton, Victoria 3169, AUSTRALIA
*Corresponding author, E-mail address: Matthew.Sinnott@csiro.au

ABSTRACT

Food transport through different sections of the gastrointestinal tract for the purposes of digestion and waste removal is an essential physiological function for life. Mechanical and chemical breakdown of food takes place throughout the intestines. Periodic muscular contraction and relaxation of the intestinal walls agitate, mix and propel the multiphase digesta along the intestines. Experimental measurement of flow inside the intestines is difficult therefore understanding of food transport through the majority of the gut is limited. Computational models for predicting the transient behaviour of intestinal content subject to peristaltic activity offer the possibility for assessing the digestive performance of different foods. We present a numerical model of multiphase flow through the duodenum. This consists of a flexible thin membrane representing the gut wall coupled to the particle-based methods Smoothed Particle Hydrodynamics (SPH) and Discrete Element Method (DEM) which are used to predict the motion of liquid and solids content respectively. The gut wall is viscoelastic and the digesta consists of solid particulates suspended in a viscous Newtonian fluid. Peristaltic waves travel along the gut wall resulting in active muscular contractions and relaxations of the gut. The influence of wall motions on transport of the liquid and solid phases is reported, as well as axial mixing of the solids. The bulk motion of the content shows both phases move together due to the laminar nature of the flow with only very short-term differences found in the relaxation region and in the wake of the contraction. The inclusion of solids mildly modifies the overall propulsive flow behaviour and the retrograde jet in the wake of the contraction. The absence of solids leads to a transverse wobbling instability in a fluid filled flexible tube which is not constrained by mesenteric connectivity.

INTRODUCTION

Partially digested food in the form of a slurry of solids and liquid exits the stomach though the pyloric sphincter (Harrison et al. 2015) and discharges into the duodenum, which is the first section of the small intestine. Gastric digestion typically reduces solid food down to 1-2 mm size fragments (Kong & Singh, 2008) which become feed for the next stages of mechanical and chemical digestion in the small intestine. The majority of enzymatic breakdown of food and significant nutrient absorption occurs in the short (roughly 25 cm) duodenal section. Following this, digesta are transported downstream into the jejunum. Bile and pancreatic juices are secreted in the duodenum and aid chemical digestion. Receptors in the duodenal wall regulate the rate at which the stomach empties (Shahidullah et al. 1975) for different food compositions. In particular, large amplitude tonic contractions of the duodenum due to the presence of acids or lipids result in delayed gastric emptying (Rao et al. 1996). In general, individual sections of the gastrointestinal (GI) tract have unique motor control and can synchronize their motor activity with neighbouring sections. This occurs throughout the GI tract except in the transition from stomach to small intestine. There is a lack of continuity in the coordination of peristaltic activity from the antrum of the stomach into the duodenum due to a lack of pacemaker cells in the pylorus (Wang et al. 2005).

Motor patterns in the first part of the small intestine are either peristaltic (propulsive in nature) or segmentative (non-propulsive and short duration). Segmentation patterns are near-stationary sequences of alternating muscular contractions and relaxations of the gut wall which are found to dominate in the presence of high nutrients such as proteins, starches and lipids when transit is required to be low for digestion (Gwynne et al. 2004). They are believed to be responsible for mixing digesta which is essential for maintaining uniform food/enzyme composition along the length of the duodenum. Although no significant evidence of their mixing ability has been demonstrated based on fluid dynamics models (de Loubens et al. 2012) they may play a role in mechanical agitation and breakdown of digesta. Conversely, propulsive patterns in the small intestine are generally believed to be more important for axial transport than mixing. Cleary et al. (2015) have demonstrated the mixing capability of a non-occluding peristaltic wave and Sinnott et al. (2012) have identified a toroidal vortex as the mechanism for this mixing.

This study uses a flexible membrane for the gut wall with peristaltic propulsive motor patterns coupled to multiphase solid/fluid slurry of digesta to investigate differences in transport through the small intestine for different content. We consider the cases of a fully liquid content and a content containing 20% particulate solids.

COMPUTATIONAL MODEL

Smoothed Particle Hydrodynamics (fluid phase)

The fluid phase of the intestinal content is modelled using the Smoothed Particle Hydrodynamics (SPH) method. This uses a meshless spatial discretisation to convert systems of PDEs into coupled systems of ODEs that can then be solved using suitable time integration

methods. See Monaghan, 2005 for a review of this method. For fluids, the continuity equation is

$$\frac{d\rho_a}{dt} = \sum_b m_b \mathbf{v}_{ab} \cdot \nabla_a W_{ab} \quad (1)$$

where ρ_a is the density of particle a with velocity $\mathbf{v}_a$ and m_b is the mass of particle b. We denote the position vector from particle b to particle a by $\mathbf{r}_{ab} = \mathbf{r}_a - \mathbf{r}_b$ and the velocity difference by $\mathbf{v}_{ab} = \mathbf{v}_a - \mathbf{v}_b$. $W_{ab} = W(\mathbf{r}_{ab}, h)$ is the interpolation kernel with smoothing length h evaluated at distance $|\mathbf{r}_{ab}|$. The SPH method used here for fluids is a quasi-compressible formulation with an equation of state specifying the relationship between particle density and fluid pressure. A form suitable for weakly compressible fluids is:

$$P = \frac{c^2 \rho_0}{\gamma}\left[\left(\frac{\rho}{\rho_0}\right)^{\gamma} - 1\right] \quad (2)$$

where P_0 is the magnitude of the pressure given by

$$\frac{\gamma P_0}{\rho_0} = 100V^2 = c^2 \quad (3)$$

and V is the characteristic or maximum fluid velocity and c is the speed of sound (Monaghan, 1994). This means that the sound speed is ten times the characteristic speed and ensures that the density variation is less than 1% and that the flow is close to incompressible. ρ_0 is the reference density and γ =7.

The SPH form of the momentum equation becomes the acceleration for each particle a:

$$\frac{d\mathbf{v}_a}{dt} = -\sum_b m_b \left[\left(\frac{P_b}{\rho_b^2} + \frac{P_a}{\rho_a^2}\right) - \frac{\xi}{\rho_a \rho_b}\frac{4\mu_a\mu_b}{(\mu_a+\mu_b)}\frac{\mathbf{v}_{ab}\cdot\mathbf{r}_{ab}}{\mathbf{r}_{ab}^2+\eta^2}\right] + \mathbf{g} \quad (4)$$

where P_a and μ_a are pressure and viscosity of particle a. Here ξ is a factor associated with the viscous term, η is a small parameter used to smooth out the singularity at $\mathbf{r}_{ab}$ = 0 and $\boldsymbol{g}$ is gravity.

Discrete Element Method (solids phase)

The particulate solids are represented here using the Discrete Element Method (DEM). This involves following the motion of every particle or object in the flow and modelling each collision between the particles and between the particles and their environment. The algorithm has three main stages:

1. A search grid is used to periodically build a near-neighbour interaction list that contains all the particle pairs and object-particle pairs that are likely to experience collisions in the short term.
2. The forces on each pair of colliding particles and/or boundary objects are evaluated in their local reference frame using a suitable contact force model, and then transformed into the simulation.
3. All the forces and torques on each particle and object are summed and the resulting equations of motion are integrated to give the resulting motion of these bodies.

The implementation used here is described in more detail in Cleary (2004, 2009). The entities are allowed to overlap and the amount of overlap Δx, and normal v_n and tangential v_t relative velocities determine the collisional forces via a contact force law. A linear spring-dashpot model is used where the normal and tangential forces are given by:

$$F_n = -k_n \Delta x + C_n v_n \quad (5)$$

$$F_t = \min\left\{\mu F_n, k_t \sum v_t \Delta t + C_t v_t\right\} \quad (6)$$

The normal force consists of a linear spring to provide the repulsive force and a dashpot to dissipate a proportion of the relative kinetic energy. The maximum overlap between particles is determined by the stiffness k_n of the spring in the normal direction. Typically, average overlaps of < 0.5% of the particle diameter are desirable. The normal damping coefficient C_n is chosen to give the required coefficient of restitution ε. The vector force F_t and velocity v_t are defined in the plane tangent to the surface at the contact point. The tangential summation term represents an incremental spring that stores energy from the relative tangential motion and models the elastic tangential deformation of the contacting surfaces, while the dashpot dissipates energy and models tangential plastic deformations. The total tangential force F_t is limited by the Coulomb frictional limit μF_n, at which point the surface contact shears and the particles begin to slide over each other.

For details of the coupling of the DEM and SPH methods for the particulate and fluid phases, see Cleary (2015).

Flexible wall model and peristaltic waves

The duodenum wall is passively compliant and can accommodate peristaltic waves of active contraction and relaxation of circular muscle. The model uses a flexible membrane representation and peristaltic wave control which are fully described in Sinnott et al. (2012). The duodenum model geometry is a cylindrical tube with closed rigid walls at each end. The curved boundary wall is viscoelastic and therefore generates tensile forces if stretched beyond its natural length in any direction. The setup of this closed tube geometry is similar to the one used by Sinnott et al. (2015) to study a lab model of a section of animal intestine for analysing manometric data from similar propulsive patterns. The tube is filled with just enough content to completely fill it ensuring that there are no void spaces and also so that there are no tensile forces generated in the walls when at rest.

The surface of the duodenum is discretized into SPH boundary particles. A viscoelastic bond is constructed between each pair of adjacent boundary particles. This consists of a linear spring (for elastic deformation) and a dashpot (for viscous damping) as defined by equations 5 and 6 for the normal direction only. In the absence of real material properties for the duodenum tissue, the stiffness of the springs was chosen to be 10 N/m and the damping coefficient of 1.9 gives a coefficient of restitution of 0.5. The extension of the springs and their motion is the result of the balance of hydrodynamic forces applied to it by the

digesta within the intestine and the viscoelastic wall force. The resulting cylindrical network of these boundary particles with wall bonds provides a compliant boundary which is able to flex in response to variations in internal content pressures. Muscular forces within the intestine wall which cause it to contract or relax are modelled by changing the natural lengths of the bonds which models the contraction of the intestine wall muscle fibres. The instantaneous shape of the wall is therefore a direct prediction from the fluid-structure interaction between content pressures and tensile wall forces.

A sequence of moving sinuosoidal peristaltic waves is generated in the intestinal wall at various locations and travel from the pylorus (oral end) towards the jejunum (anal end). Each wave consists of a contraction region with a leading relaxation region that is in advance of the contraction. These influence the instantaneous wall tensions in each longitudinal slice of the duodenum wall. The operation of the model emulates the real behaviour of propulsive motor patterns in the intestines.

Biomechanical model of the duodenum and content

The duodenum geometry used in this study is (at rest) a closed cylindrical tube with diameter 2.5 cm and an axial length of 25 cm as shown in Figure 1. In vivo, the oral end of the real duodenum is closed due to constriction of the pylorus but the downstream end leading into the jejunum is open. Instead, the model in this paper represents an in vitro lab preparation of a section of intestine with tied ends similar to a previous study (Sinnott et al. 2015). This geometry is filled with a stationary Newtonian fluid having a density of water (1000 kg/m^3) and viscosity of 0.01 Pa.s. Content have a broad range of viscosities inside the small intestine due to differences in food composition. For example dietary fibre is known to increase content viscosity (Dikeman et al. 2006). Therefore we choose values here to reflect representative properties of a typical liquid phase in the duodenum. The SPH model uses a fluid resolution of 1.25 mm giving 110,000 SPH particles in the domain. The boundary spacing of 0.625 mm is finer so that the maximum separation between boundary particles at peak relaxation remains smaller than the SPH fluid resolution giving 53,000 boundary particles. The dispersed particulate solid phase consists of 1 mm diameter neutrally buoyant DEM spheres (representative of typical particle sizes following gastric digestion). Two cases are investigated in this study for different content:

1) a fluid only case; and
2) a multiphase slurry case which contains 20% solid loading in the 1st half of the duodenum (as shown in Figure 1) with fluid only in the latter half.

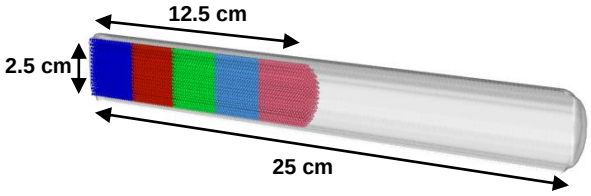

Figure 1: Duodenum geometry (grey) with closed ends. Particulate solids occupy the first half of the tube and are coloured as axial bands according to their initial position.

Particles are coloured into axial bands based on their starting position along the duodenum. This provides a visual way of tracking the mixing and transport of the solids content. Computation timesteps of 4.7x10^{-5} s and 4.3x10^{-5} s are used for the fluid only and multiphase simulations respectively.

Peristaltic waves are set up in the duodenal wall with a duration of 5 s and wave speed of 2 cm/s. These commence at the same location (5 cm from the start of the tube) for each wave and repeat every 6 s for a total series of 10 waves, allowing 1 s of relaxation time in between successive waves. The period was chosen so that the wave dissipates well before approaching the closed anal end of the tube so that downstream pressures near the closed end do not become excessively high. An 80% shortening of elastic wall elements define the maximum active contraction while a matching 80% lengthening of the elements define the maximum active relaxation of the wall. The axial length of the full wave (including both contractile and relaxation parts) is 8 cm.

RESULTS

Fluid Only

Figure 2 shows the flow field for the fluid only content at different times during the passage of the 1st peristaltic wave along the length of the duodenum. This shows the deformation of the wall and the fluid content both coloured by axial speed. The wave travels from left (oral end) to right (anal end).

At 1.5 s (Figure 2a), the contraction and relaxation components are substantially developed. High axial speeds (red) up to 50% greater than the wave speed occur at the centre of the relaxation region. Here the walls dilate due to the high pressures generated in front of the advancing contraction (see Sinnott et al. 2015 for the relationship between pressure field and axial velocities). Near the wall, speeds are lower (green) at roughly half of the wave speed. This radial dependence on axial speed results in a toroidal vortex (discussed in detail in Sinnott et al. 2012 in the context of transport of viscous liquid in the large intestine) inside the relaxation region which is important for radial transport of nutrients to the wall for absorption as well as radial and axial mixing of content.

At 3 s (Figure 2b) the relaxation region is now less elongated in the axial direction and more spherical in shape and the flow field inside is more symmetrical. A strong fully developed jet is present inside the contraction region. This reverse jet is important for redistributing content back along the length of the duodenum and for the re-pressurization of the duodenum walls near the oral end.

At 4.5 s (Figure 2c) the wave has nearly finished dissipating and the previous flow pattern is rapidly decaying so that flow is now entirely in the reverse direction. Downstream pressures near the closed anal end of the tube relax and content axially redistributes back towards the oral end. Due to the closed ends there is no net axial flow inside this model as a consequence. This restricts the degree of axial transport for the particulate solids in the next section but results in enhanced mixing of the solids in the first half of the tube.

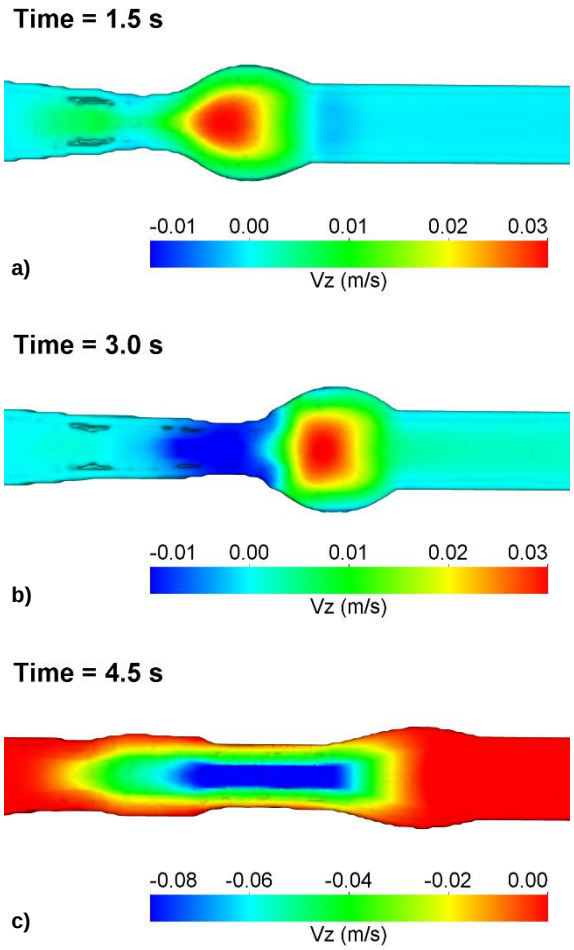

Figure 2: The passage of a single peristaltic wave along the length of the duodenum for fluid only content. Fluid is coloured by axial speed.

Slurry of 20% particulate solids

The inclusion of 20% fine particulate solids into the fluid content produces some small scale but interesting changes to the propulsive transport. Figure 3 shows the passage of a similar peristaltic to that shown in Figure 2 and at the same times for easy comparison. In addition, the distribution of particulate solids along the axial length of the tube is shown at each time. The Reynolds number (Re) for the fluid is 80 and for the solids is 1.5 and therefore both phases are laminar. Since the particle Re is small, there is little opportunity for the fluid and solids phases to move differentially during the passage of a contraction wave. However, the combined solids/liquid flow field shows some differences to the fluid only case.

At 1.5 s (Figure 3a), the peak fluid speed inside the relaxation region is reduced relative to the fluid only case and the size of the high speed flow region shrinks. Fluid content in the wake of the contraction occupies a central region whereas the solids tend to spread sideways towards the wall. Mixing of the solids occurs by stretching of content in the axial direction propelled downstream by the passage of the peristaltic wave. Transverse folding of the solids then occurs within the toroidal vortex in the relaxation region. Here the green/blue solids migrate to the wall and are dragged behind the wave by low axial fluid speeds at the wall. This results in a radial layering of the coloured bands of particles after the passage of each wave.

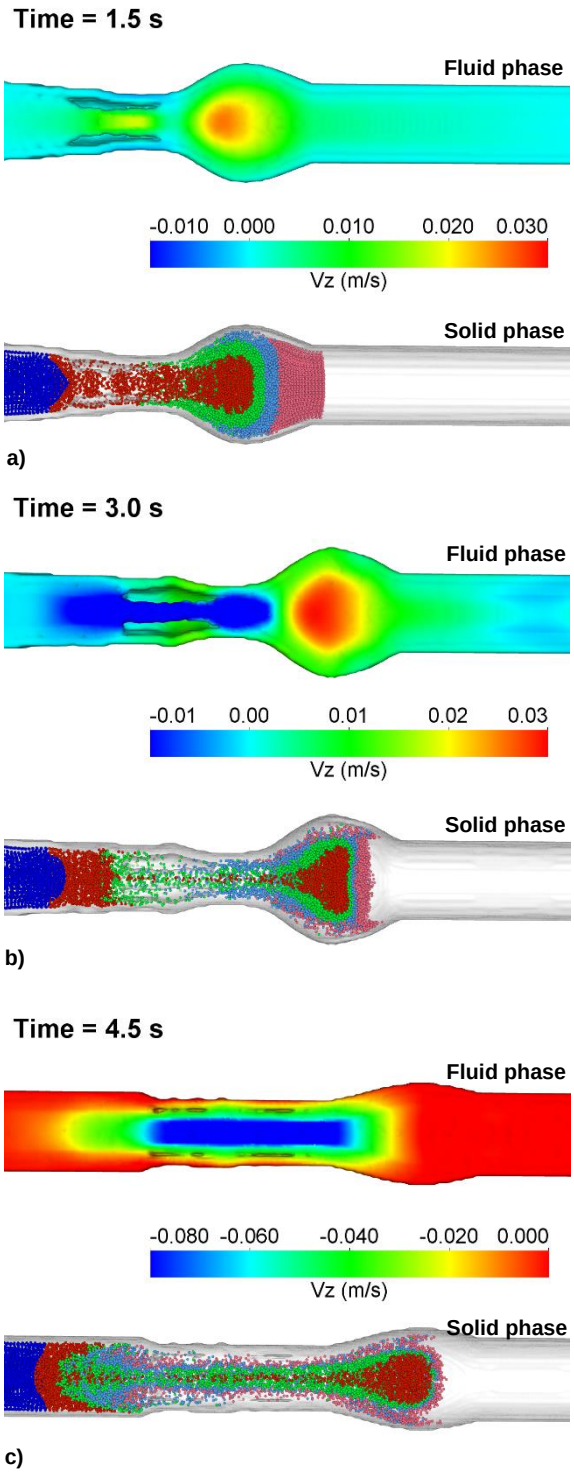

Figure 3: The passage of a single peristaltic wave along the length of the duodenum for content with 20% solids loading at three different times. The top picture at each time shows fluid phase coloured by axial speed. The bottom picture at each time shows the solids coloured by their initial position.

At 3 s (Figure 3b), the fluid flow field inside the relaxation region is very similar to the fluid only case but the shape of the dilated wall is slightly different (the trailing edge near the contraction is slightly steeper in gradient) indicating that the pressure distribution along the duodenal wall is modified by the presence of the solids. The reverse jet from the rear of the contraction region is

not as strong as for the fluid only case. It jet is narrower and more centralised. Inside the relaxation region, the solids are more centrally located and are only sparsely distributed near the expanding wall. The mixing of the solids has developed further with radial migration of the pink particles to the walls as well as extending back to the contraction region.

By 4.5 s (Figure 3c) the radial layering of the solids extends along almost the full axial length of the duodenum. The convergence of the wall upstream of the contraction takes longer to relax back to its original diameter which indicates that fluid pressures take longer to equilibrate upstream as a consequence of the reduced strength in the reverse flow caused by the presence of the solids.

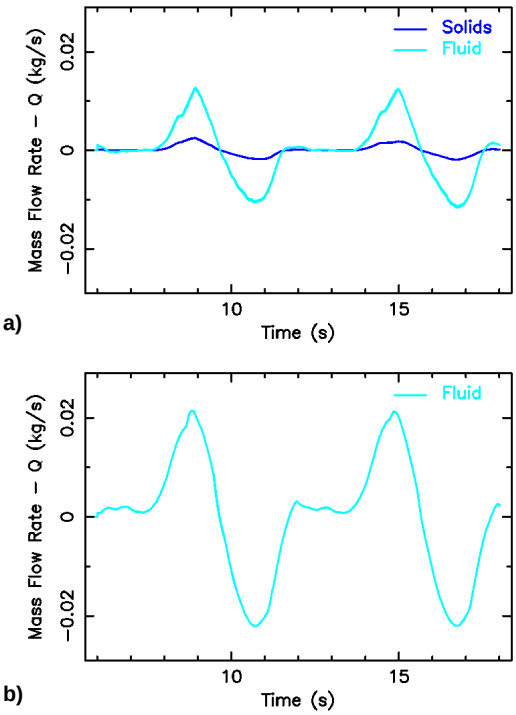

Figure 4: The time variation of the mass flow rates measured halfway along the length of the duodenum. The flow rates are shown for peristaltic waves 2 and 3 for: a) 20% solids loading, and b) fluid only content.

Figure 4 compares the mass flow rates for the multiphase and fluid only cases. These are measured at a vertical cross-sectional data collection plane located halfway along the length of the model duodenum. The peak mass flow rate of the total solid/liquid content is ~1/5 lower than the peak rate for the fluid only case. The solids phase contributes roughly 20% to the overall peak mass flow rate which is consistent with the 20% solids loading by mass for the neutrally buoyant material.

Figure 5 shows the axial flow velocities spatially averaged over the data collection plane used for Figure 4 for the multiphase and fluid only cases. For the multiphase case, the average velocities for the solid and fluid phase are almost identical for the majority of the period of each wave indicating that the two phases are strongly coupled together for most of the time. However, inside the relaxation region the solids have higher forwards velocities of 30 mm/s compared to speeds of 10 - 20 mm/s for the fluid phase. This is mostly a consequence of the radial distribution of the solids inside the relaxation region since they are more sparsely distributed near the wall. Therefore more of the solids are located in the high velocity central flow region (see Figure 3b). The low fluid Reynolds number could lead to the interpretation that the solids completely move with the fluid, however there are some short-term differences between phases which may impact on the digestion of the solids and diffusion of resulting species to the wall for absorption. The peak retrograde velocities for the fluid only case are about 90% higher in the absence of solids. This results in transverse motion of the duodenum wall and is the focus of the next section.

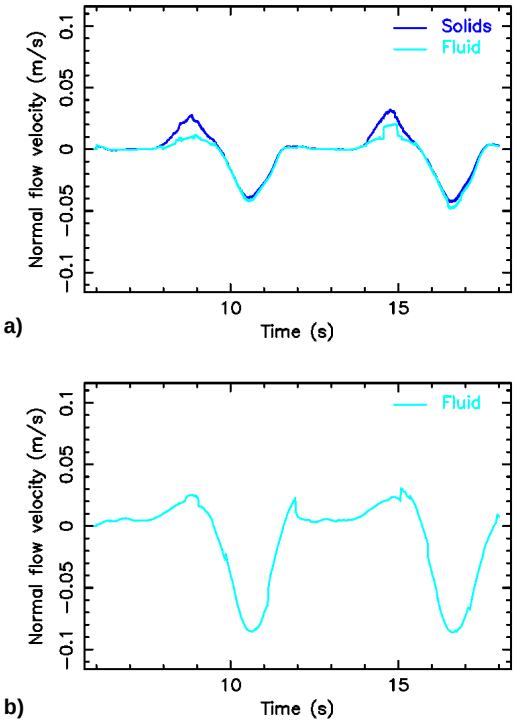

Figure 5: The time variation of the average axial velocities crossing a plane located halfway along the length of the duodenum. The velocities are shown for waves 2 and 3 for: a) 20% solids loading, and b) fluid only content.

Low pressure induced “wobbling” instability

For fluid only content, the duodenum experiences significant transverse mobility in the reduced pressure region in the wake of each of the peristaltic waves (see Figure 6). There is a residual low pressure region that is generated in the wake of the compression zone of the contracting wall. This persists for a reasonable time as it takes time for the viscous fluid to flow back towards the oral end in response to the weak axial pressure gradient and to equilibrate the pressures in the system. This can be characterised as a relaxation process for the system. During this time while the flexible wall behind the contraction is not fully pressurised it becomes subject to a transverse “wobbling” instability. The instability develops after 5-6 waves have traversed the duodenum.

Figure 6a&b show the first second of waves 7 and 8 while Figures 6c&d show one second before the end of waves 8 and 9. They show the degree of vertical movement in the walls which oscillate transversely with a

period that is longer than the period of the peristaltic waves (which reflects the long relaxation time of the system).

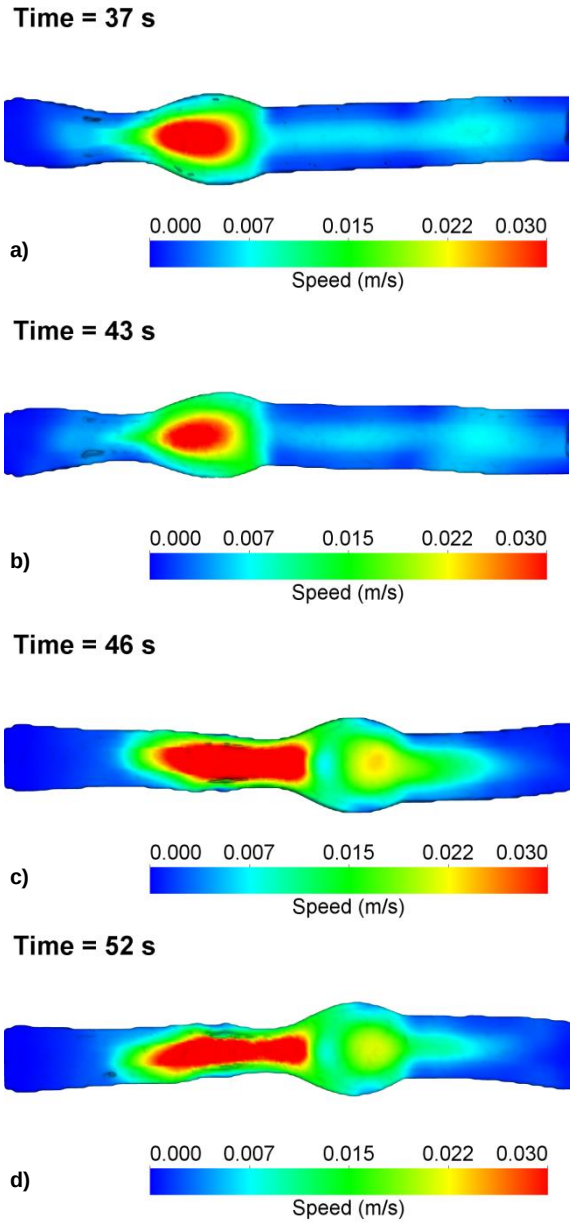

Figure 6: A transverse wobbling instability observed in the fluid only case. It begins to develop after the passage of several peristaltic waves.

This wobbling instability arises because there is not sufficient overpressure in this part of the tube to increase pressures in the wake of the contraction. If one wanted, this instability could be inhibited by increasing the fluid pressures in the tube.

For the 20% solids loading case the instability does not manifest with no transverse movement after 10 wave passages. This indicates that the presence of reasonable solids loading in the wake of the contraction is sufficient to inhibit the development of the instability.

Based purely on the model it is not possible to determine if the instability is physical or numerical or a combination. It is not unreasonable that an unsupported depressurized relaxed tube with strong internal fluid forces applying elsewhere in the tube could be subject to a physical transverse instability. If this is true, a complicating factor is that the movement of the intestines are restricted with attachments within the abdomen via thin connective tissue called the mesentery which will moderate such movements. Connective tissue restraints will therefore be incorporated into future models of the intestines.

CONCLUSION

The response of liquid and solid/liquid slurry content to propulsive peristaltic waves has been investigated for a closed compliant section of the start of the small intestine. Purely liquid content is propelled forwards inside the relaxation region and a retrograde jet redistributes content axially back towards the oral end. This results in re-pressurization of the oral end of the tube back to its original diameter once the wave has dissipated.

The presence of solids modifies the fluid pressures in the relaxation region mildly changing the dilated wall shape and fluid flow field. The propulsive wave results in strong axial mixing of the solids content along much of the length of the duodenal section.

A transverse wobbling instability can develop inside the residual low pressure region in the wake of each contraction. The walls of the duodenum oscillate at a period greater than the period of the peristaltic waves due to the long relaxation time of the system. This instability is a consequence of the absence of mesenteric connective tissue attachments in the model and one could inhibit this by including these attachments or by adding overpressure to the model to increase fluid pressures behind the contraction. The presence of a solid phase in the content was found to damp out this instability by reducing the strength of the retrograde jet.

REFERENCES

CLEARY, P.W., (2004), "Large scale industrial DEM modelling", *Engineering Computations* **21(2/3/4)**, 169-204.

CLEARY, P.W., (2009), "Industrial particle flow modelling using discrete element method", *Engineering Computations* **26(6)**, 698-743.

CLEARY, P.W., (2015), "Prediction of coupled particle and fluid flows using DEM and SPH", *Minerals Engineering* **73**, 85-99.

CLEARY, P.W., SINNOTT, M.D., HARI, B., BAKALIS, S., AND HARRISON, S.M., (2015), "10 - Modelling food digestion", in: Fryer, S.B.K.J. (Ed.), *Modeling Food Processing Operations*, Woodhead Publishing Series in Food Science, Technology and Nutrition. Woodhead Publishing, pp. 255–305.

DE LOUBENS, C., LENTLE, R.G., LOVE, R.J., HULLS, C., AND JANSSEN, P.W., (2013), "Fluid mechanical consequences of pendular activity, segmentation and pyloric outflow in the proximal duodenum of the rat and the guinea pig", *Journal of The Royal Society Interface* **10(83)**, 20130027.

DIKEMAN, C.L., MURPHY, M.R., AND FAHEY, G.C., (2006), "Dietary fibers affect viscosity of solutions and simulated human gastric and small intestinal digesta", *The Journal of nutrition* **136(4)**, 913-919.

GWYNNE, R.M., THOMAS, E.A., GOH, S.M., SJÖVALL, H., AND BORNSTEIN, J.C., (2004),

"Segmentation induced by intraluminal fatty acid in isolated guinea-pig duodenum and jejunum", *The Journal of Physiology* **556**, 557–569.

HARRISON, S.M., CLEARY, P.W., AND SINNOTT, M.D., (2015), "Investigating stomach mixing and emptying for aqueous liquid contents using a coupled biomechanical-Smoothed Particle Hydrodynamics Model", *Proc: 11th Int Conf on CFD in the Minerals and Process Industries*, Melbourne, Australia. ID: 123HAR.

KONG, F., AND SINGH, R.P., (2008), "Disintegration of solid foods in human stomach", *Journal of food science* **73(5)**, R67-R80.

MONAGHAN, J.J., (1994), "Simulating free surface flows with SPH", *Journal of computational physics* **110(2)**, 399-406.

MONAGHAN, J.J., (2005), "Smoothed particle hydrodynamics", *Reports on progress in physics* **68(8)**, 1703-1759.

RAO, S., LU, C., AND SCHULZE-DELRIEU, K., (1996), "Duodenum as a immediate brake to gastric outflow: A videofluoroscopic and manometric assessment", *Gastroenterology* **110**, 740–747.

SHAHIDULLAH, M., KENNEDY, T.L., AND PARKS, T G., (1975), "The vagus, the duodenal brake, and gastric emptying", *Gut* **16(5)**, 331–336.

SINNOTT, M.D., CLEARY, P.W., ARKWRIGHT, J.W., AND DINNING, P.G., (2012), "Investigating the relationships between peristaltic contraction and fluid transport in the human colon using Smoothed Particle Hydrodynamics", *Computers in biology and medicine* **42(4)**, 492-503.

SINNOTT, M.D., CLEARY, P.W., DINNING, P.G., ARKWRIGHT, J.W., AND COSTA, M., (2015), "Interpreting manometric signals for propulsion in the gut", *Computational Particle Mechanics* **2(3)**, 273-282.

WANG, X.Y., LAMMERS, W.J., BERCIK, P., HUIZINGA, J.D., (2005), "Lack of pyloric interstitial cells of Cajal explains distinct peristaltic motor patterns in stomach and small intestine", *American Journal of Physiology-Gastrointestinal and Liver Physiology* **289(3)**, G539-G549.

